6th International Symposium on Solid Mechanics

Click on the box to select the Mini-Symposia:

- ☒ Multiaxial and Fretting Fatigue (*Edgar Mamiya* and *Lucival Malcher*);
- ☐ Composite Materials (*Ricardo de Medeiros*);
- ☐ Constitutive Models I – Plasticity and Damage (*Lucival Malcher*, *Miguel Vaz Jr.* and *Edgar Mamiya*);
- ☐ Constitutive Models II – Viscoelastic and Viscoplastic Solids: Models and Applications (*Heraldo Mattos*);
- ☐ Impact Engineering (*Marcílio Alves*);
- ☐ Structural Reliability Methods and Reliability-Based Design Optimization (*André Beck*);
- ☐ Topology Optimization of Multifunctional Materials, Fluids and Structures (*Eduardo Lenz Cardoso* e *Emilio Carlos Nelli Silva*);
- ☐ Topological Derivatives: Theory and Applications (*André Novotny*);
- ☐ X-FEM, G-FEM and Meshfree Methods (*Roberto Dalledone Machado* and *Rodrigo Rossi*);
- ☐ High Order Finite Elements (*Marco Lúcio Bittencourt*);
- ☐ Nonlinear Analyses (*Eduardo Campello*);
- ☐ Other section;

MECSOL Joinville 2017

April 26-28, 2017
Joinville, Santa Catarina, Brazil

Fatigue Analysis of a Compact Tension Specimen with Multiple Micro-cracks/voids Repaired by Stop-hole Technique

Mohammad Malekan
Graduate Program in Structural Engineering (PROPEEs)
School of Engineering, Federal University of Minas Gerais (UFMG)
malekan@dees.ufmg.br, mmalekan1986@gmail.com

Felicio B. Barros
Graduate Program in Structural Engineering (PROPEEs)
School of Engineering, Federal University of Minas Gerais (UFMG)
felicio@dees.ufmg.br

Hermes Carvalho
Graduate Program in Structural Engineering (PROPEEs)
School of Engineering, Federal University of Minas Gerais (UFMG)
hermes@dees.ufmg.br

ABSTRACT

From the engineering point of view there are traditionally two ways to approach the fatigue design problem: safe-life and damage-tolerant. The damage-tolerant methodology focus on predictions of the fatigue crack growth rate and the remaining fatigue life whereas the safe-life design methodology focuses on estimating the total life. Thus, estimations of the remaining fatigue life of a flawed structure is only possible through use of the damage-tolerant approach. Fatigue is a process in engineering materials in which damage accumulates due to the fluctuating loading. One solution for a component under the fatigue process is to arrest the crack growth before the final failure using different available retardation methods. This paper aims to investigate the effect of the stop-hole retardation technique and multiple micro-cracks/voids on the fatigue crack growth (FCG) in a compact tension specimen. Considering the linear elastic fracture mechanics concept, the Paris law will be used to define the transition between crack initiation and crack growth period. Also, the extended finite element method will be adapted in the crack propagation phase in order to exclude the remeshing procedure. The whole analyses are conducted in a commercial package along with some user-written codes to make the FCG process easier. The reference solutions from the literature are used to compared and validate the results obtained from the current research.

Keywords: Fatigue Analysis, Crack Retardation, Finite Element Method, Voids

1 INTRODUCTION

One of the failure modes in engineering problems is the fatigue fracture. This phenomena starts with initiation and propagation of a crack which results in the component final. Different industries such as aerospace and machinery are dealing with the fatigue phenomena and cause them a great economic loss every year. One solution for a component under the fatigue process is to replace that with a new one, but in most of the times it requires significant amount of time and is costly. Another solution is to arrest the crack growth before the final failure using different available methods.

One of the easiest and most accessible crack arresting methods is drilling holes close to the crack tip [1]. This method helps to changing the crack growth direction and also for retarding the

fatigue crack propagation, either by a single hole or two symmetric holes with respect to the crack surface [2-4]. More recently, Ayatollahi et al. [1, 5] studied the effect of stop hole drilling on the fatigue life extension under different fracture modes conditions. Their numerical model was able to predict the fatigue life extension of the repaired specimens.

Behavior of the structures with a main crack may varies in the presence of micro-defects as they can change the mechanics of fracture in the medium of the structure. In many cases such as quasi-brittle materials, one macro-crack simultaneously interacts with several micro-cracks/voids. This interaction demands a complex numerical approach to extract fracture parameters such as stress intensity factor (SIF). There are many researches dealing with macro-crack interactions. Soh and Yang [6] presented a hybrid-type special finite element using a conformal mapping technique in order to study the interaction between a macro-crack and a cluster of micro-defects. Other researches on analytical solution of macro-crack interacting with micro-crack(s) can be found in [7−10].

There are a few researches on the effect of micro-cracks/voids on fatigue crack propagation: Bhardwaj et al [11] presented an approach to predict the fatigue life of an interfacial cracked plate in the presence of flaws by a combination method of homogenized extended finite element method (FEM) and isogeometric analysis, called XIGA, and O'Hara et al [12] discussed a two-scale generalized FEM approach to solve fracture mechanics and fatigue crack propagation problems. In their model, both macro- and micro-crack surfaces modeled only in the local problem using the discontinuous and singular enrichment functions. Based on authors' knowledge, no studies exist in the literature regarding the fatigue crack growth behavior of the repaired specimens with stop-hole technique along with micro-cracks/voids. Therefore, the aim of present paper is to study the effect of both micro-cracks/voids and stop-hole on the fatigue life of cracked specimens. For this purpose, the fatigue crack initiation and fatigue crack growth were modeled to investigate the behavior of the repaired specimens along with micro-cracks and voids. Fatigue analyses are performed using *Python* scripting code based on the classical fracture mechanic models linked with ABAQUS commercial package.

2 FATIGUE ANALYSIS BASED ON COMPUTATIONAL METHODS

An important push to understand the fatigue process was made by Paris [13, 14], in which they found a quite linear correlation on double logarithmic scales between crack growth rate da/dN and cyclic stress intensity factor ΔK for some part of the fatigue curve. This well-known Paris' law is:

$$\frac{da}{dN} = C\Delta K^m \tag{1}$$

where *C* and *m* are experimentally determined scaling constants and *dN* is the loading cycle increment. Although this equation has no physical basis and it was derived from curve fitting, it is widely used and it has been shown to produce accurate results [15]. Both parameters are material properties. Parameter *m* describes how sensitive a material's growth rate is to the stress applied. The constant *C* is more dependent on the material [15]. Table 1 presents Paris coefficients for Aluminum 7075-T6 alloy.

Table 1: Paris equation coefficients for Aluminum 7075-T6 [16, 17]

$\boldsymbol{R-ratio}$	$\boldsymbol{C}\left(\frac{mm/cycle}{(MPa\sqrt{mm})^{m}}\right)$	$\boldsymbol{m}$
0.0	9.83×10^{-14}	3.64
0.2	4.72×10^{-15}	4.13
0.3	2.86×10^{-13}	3.59
0.5	3.40×10^{-13}	3.64
0.7	3.55×10^{-14}	4.14
0.8	3.86×10^{-15}	4.68
average	$\mathbf{2.13 \times 10^{-13}}$	$\mathbf{3.21}$

Fatigue is a process of local strength reduction. The phenomenon is often referred to as a process of damage accumulation in a material undergoing fluctuating loading. This process occurs in engineering materials such as metallic alloys, polymers and composites. To describe the mechanical fatigue process as a result of a repeated load working on a part of a structure, different parameters are used, like: cyclic load, stress intensity and crack growth rate. The maximum load is P_{max}, the minimum P_{min} $[N]$ and the ratio between the minimum and maximum load (P_{min}/P_{max}), that is often used as a measure of the mean stress, is called the load ratio R. Crack growth rate da/dN is the crack increment da per loading cycle increment dN. The stress intensity factor, K $[MPa\sqrt{m}]$, working on the crack tip is calculated from the applied load P and actual crack length and direction in a construction. The maximum stress intensity is K_{max}, the minimum K_{min} and the difference between them is ΔK, see Figure 1.

Fluctuating loads can lead to fluctuating local high stresses and microscopic small cracks may appear. Once a crack exists in a structure, it will tend to grow under cyclic loading. Even if the maximum of the cyclic load on a construction is below the elastic limit of the material, fatigue may lead to failure. Fatigue is a progressive process, the damage develops slowly in the early stages and near the end of a structure's life it accelerates very quickly towards failure.

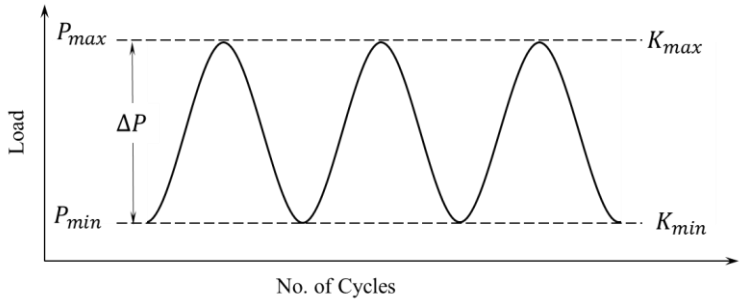

Figure 1: Loading parameters to describe the fatigue loading

The crack growth direction, θ_c, is obtained based on the maximum tangential stress criterion [18], defined as:

$$\theta_c = 2\tan^{-1}\left(\frac{1}{4}\left[\frac{K_I}{K_{II}} \pm \sqrt{\left(\frac{K_I}{K_{II}}\right)^2 + 8}\right]\right) \tag{2}$$

where K_I and K_{II} are stress intensity factors of mode-I and mode-II fractures. An equivalent SIF, ΔKeq, is used to represent the mixed-mode conditions as [19]:

$$\Delta K_{eq} = \Delta K_I \cos^3\left(\frac{\theta_c}{2}\right) - 3\Delta K_{II} \cos^2\left(\frac{\theta_c}{2}\right) \sin\left(\frac{\theta_c}{2}\right) \tag{3}$$

with:

$$\Delta K_I = K_{I,max} - K_{I,min} \tag{4}$$

$$\Delta K_{II} = K_{II,max} - K_{II,min} \tag{5}$$

In which $K_{I,max}$ and $K_{I,min}$ are stress intensity factors for maximum and minimum loading magnitudes, for mode-I fracture. Similar expressions goes for mode-II in Eq. (5). An incremental equation for fatigue crack growth in a linear elastic regime is adopted for a step time *i*. Having the crack increment, Δa, the number of loading cycles to reach this crack increment is estimated as following, using the Paris Eq. (1):

$$N_i = N_{i-1} + \frac{\Delta a}{C\left(\Delta K_{eq}\right)^m} \tag{6}$$

and the crack length for the next iteration is determined using:

$$a_i = a_{i-1} + \Delta a \tag{7}$$

3 FINITE ELEMENT MODELING PROCEDURE

The elastic stress, strain and displacement fields of the problem were obtained using the commercial FE program ABAQUS. Then, a *Python* script is written in order to perform the fatigue crack growth automatically based of descriptions and formulations of the previous section. Actually, this approach is a recursive method to propagate the crack step-by-step.

Figure 2 shows flowchart for current implementations of the fatigue crack growth, FCG, process. This procedure starts with an elastic solution performed for the problem with an initial crack configuration. Afterwards, the incremental stress intensity factors, ΔK_{eq}, crack growth direction angles, and number of cycles for current crack extension are calculated. Then, the new crack-tip is calculated and geometry is updated for the next incremental step. This procedure continues until maximum number of steps were defined by the user.

4 NUMERICAL RESULTS

The current fatigue crack growth analysis was first validated using a stress intensity factor calculation along with crack propagation technique for an edge crack problem shown in Figure 3(a). Figure 3(b) clearly shows that SIF calculations for this kind of problems are delivering accurate results, less than 5% error comparing with the analytical solution from [20], i.e. $K_I = 1.12\sigma\sqrt{\pi a}$. Moreover, the results of an experimental a crack specimen made of Aluminum 7075-T6, reported in [21], will be reproduced numerically here, as shown in Figure 4. This second example is brought to validate the crack path calculation procedure. The crack propagation orientation is obtained using the

Eq. (2), ABAQUS only delivers the SIF values, i.e. K_I and K_{II}. Fatigue crack growth takes place under mixed mode condition, since the crack is not along the symmetry plane. A plane strain state is considered for the finite element analysis with the thickness of 16 mm. The mechanical and loading properties are shown in Table 2.

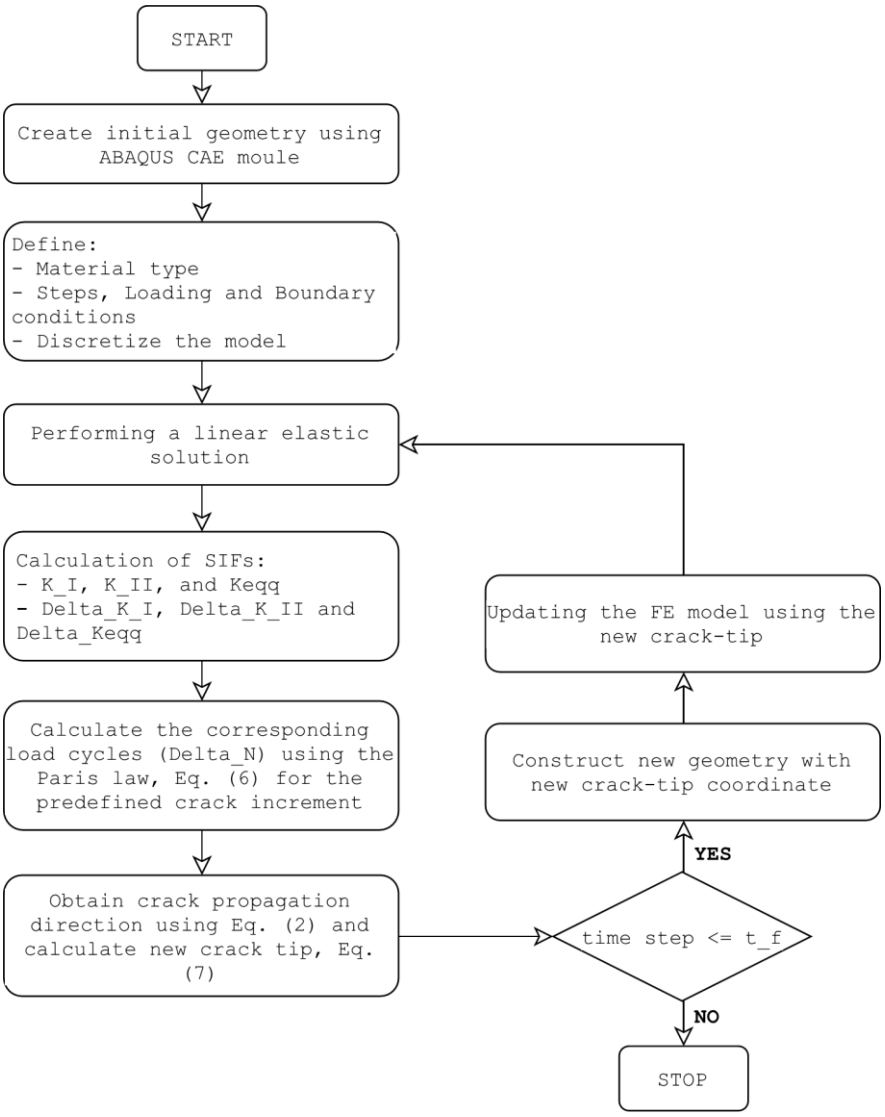

Figure 2: Fatigue crack propagation flowchart.

Table 2: Mechanical and loading properties of the test specimen [16]

$E\ (GPa)$	ν	$\rho\ (kg/m^3)$	$\sigma_{ult}\ (MPa)$	$\sigma_{yld}\ (MPa)$	R	$P\ (kN)$	$K_{IC}\ (MPa\sqrt{m})$
71.7	0.33	2780	572	518	0.1	20	44.4

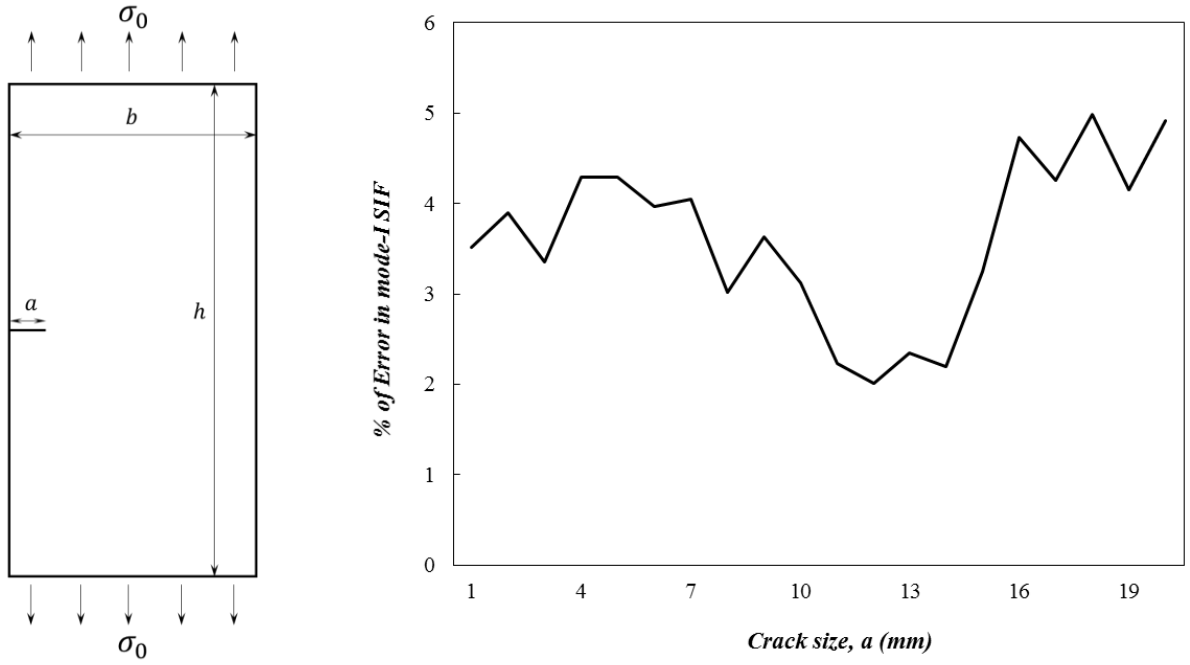

(a) (b)

Figure 3: Edge crack problem: (a) geometry with $h = 20, b = 10, a = 5,$ and $\sigma_0 = 10\ KPa$, (b) current simulation result for SIF calculations. All dimensions are in mm and Material is Aluminium 7075-T6.

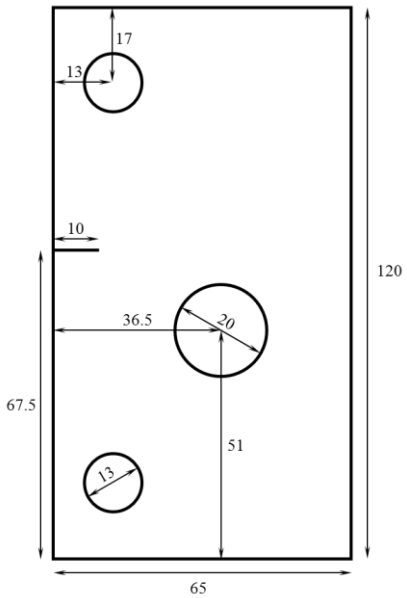

Figure 4: Geometric dimensions of the specimen [21], all dimensions are in mm.

Figure 5 shows the numerical results obtained from the current work compared with the experimental one from [21]. It can be seen from this figure that the numerically predicted path is in good agreement with the experimentally crack path result.

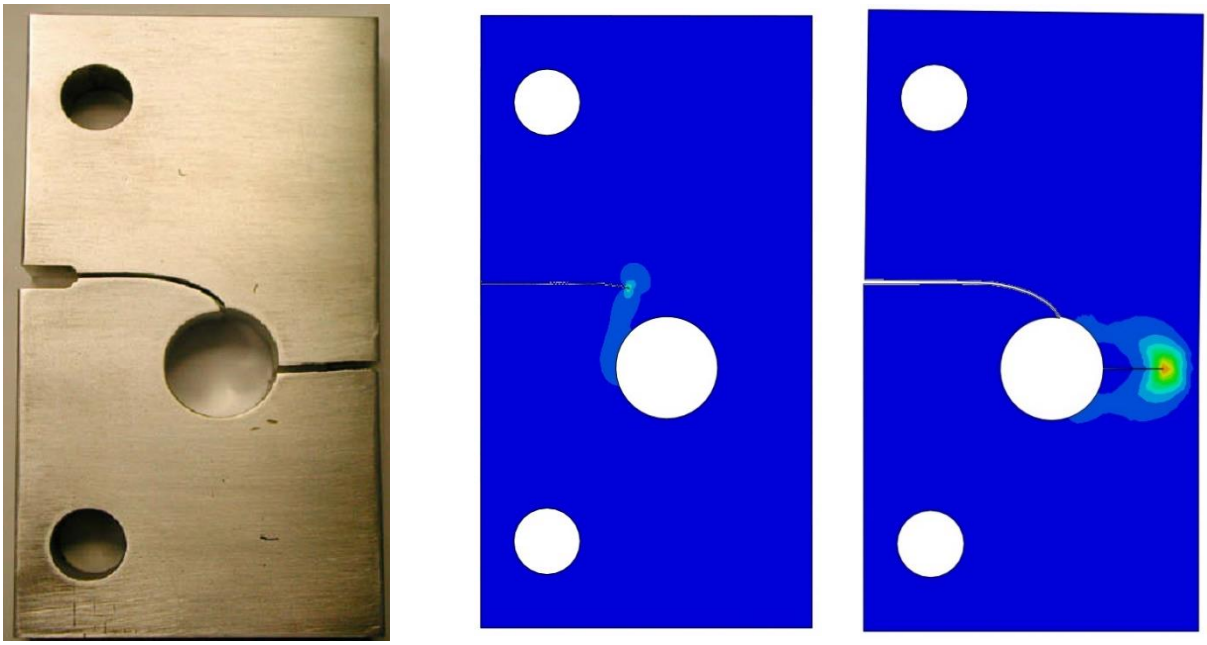

(a) (b) (c)

Figure 5: Fatigue crack growth validation: (a) experimental test result [21], (b) and (c) current simulation result for two different time steps

A compact tension specimen of thickness 9.6 mm, width $W= 50$ mm and initial crack length $a = 25mm$ was considered for fatigue analysis with linear elastic behavior assumption. A circular hole was considered at the crack tip. Figure 6 illustrates the geometry of specimen along with specifications of the stop-hole and micro-cracks.

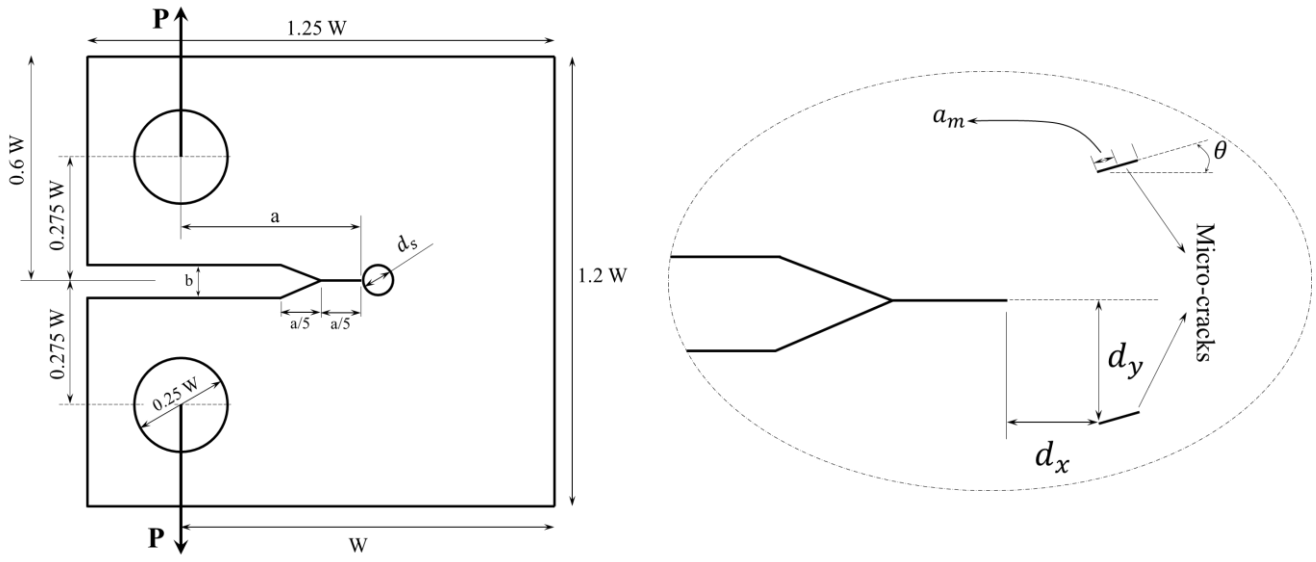

(a) (b)

Figure 6: Geometry of the compact tension specimen: (a) standard specimen, (b) stop-hole and micro-cracks geometries and locations with respect to the fatigue crack. With $b = 2, W = 50, a = 25, P = 4300N, d_s = 2$ (All dimensions are in mm).

The specimen was assumed to be made from a 7075-T6 aluminum alloy. The fatigue analyses were conducted under constant amplitude fatigue loading at the load ratio of $R = 0.1$. The diameter of stop-hole is considered to be 2 mm. The maximum level of applied cyclic loading of $P = 4.3\ kN$ were considered in the analyses. For CT specimen with stop-hole, following [1], the fatigue crack was considered to initiate from the element with the lowest fatigue initiation life in the stop-hole edge. A radial crack of 0.2 mm length was considered in the position of the element with lowest fatigue initiation life, as shown in Figure 7. Initial results for CT specimen without with and without stop-hole are shown in Figure 8.

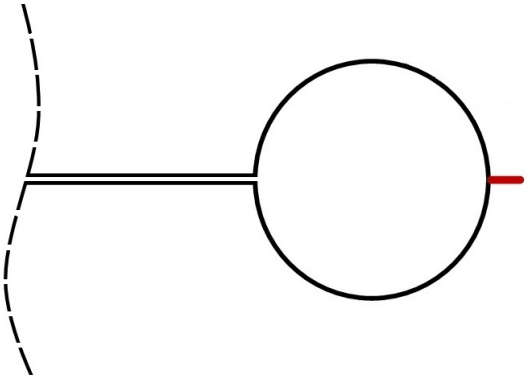

Figure 7: Location of fatigue crack initiation from the hole.

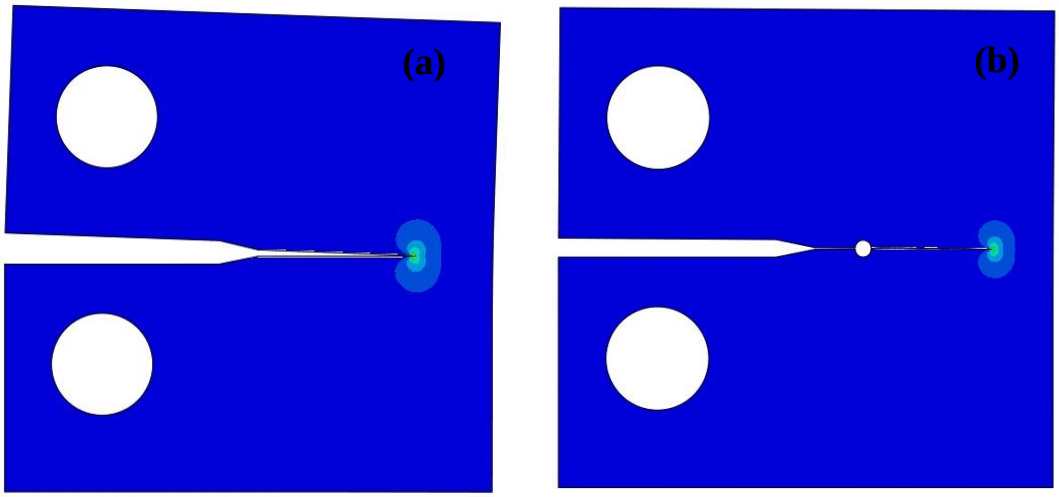

Figure 8: Fatigue crack growth path for: (a) standard specimen, (b) specimen repaired with a stop-hole.

The characteristic length of the micro-cracks/voids, a_m, were selected in such a way to have $\frac{a_m}{a} = \frac{1}{50} \leq 1$, in which a is the fatigue crack length. This characteristic length represents the half-length of the main diagonal of elliptic void and half length of the micro-crack. The characteristic lengths and direction angles, θ, for both micro-cracks/voids are the same. The horizontal distance of the micro-cracks/voids center from the main crack-tip is considered equal to $d_x = 0$. There are two vertical distances of the micro-cracks/voids center from the main crack-tip: $d_y = 1$ and 2 mm. Also, three different direction angles are considered as: $\theta = 0, 45, 90$ degrees. These two values for vertical distance and different direction angle parameters are considered in order to study the effect of them on the fatigue crack propagation configuration of the main crack. Figure 9 and Figure 10 present the

fatigue crack propagation path of the main crack interacting with two micro-cracks/ellipses, considering two vertical distances and three direction angles, for standard specimen and repaired specimen with stop-hole technique, respectively. Horizontal and vertical axes represent the coordinate of the crack front in *x*- and *y*-direction, respectively.

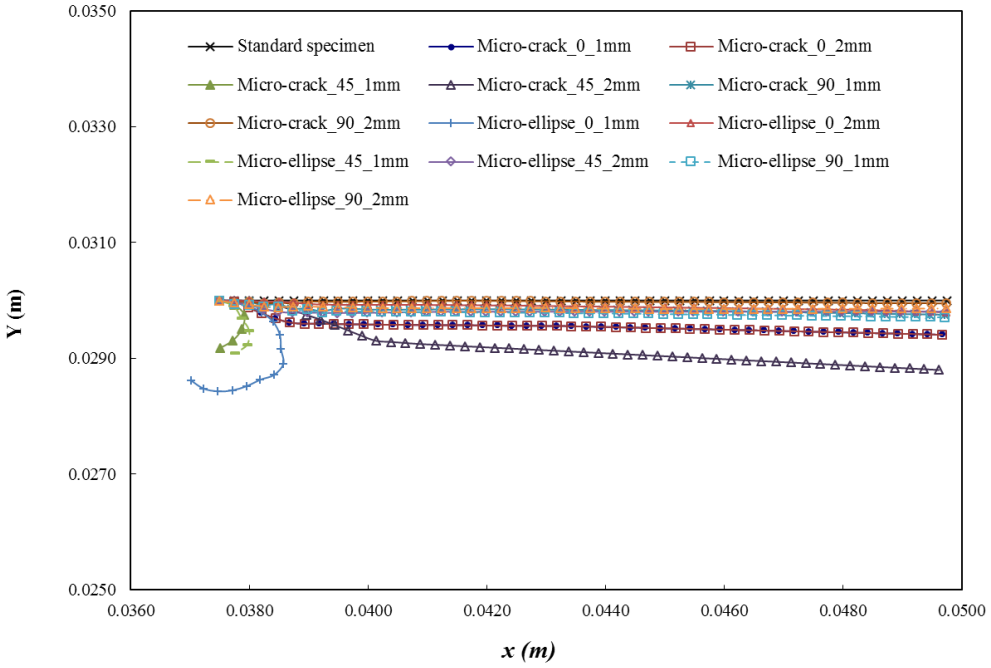

Figure 9: Fatigue crack growth path of main crack interacting with two micro-cracks/ellipses, for different d_y and θ.

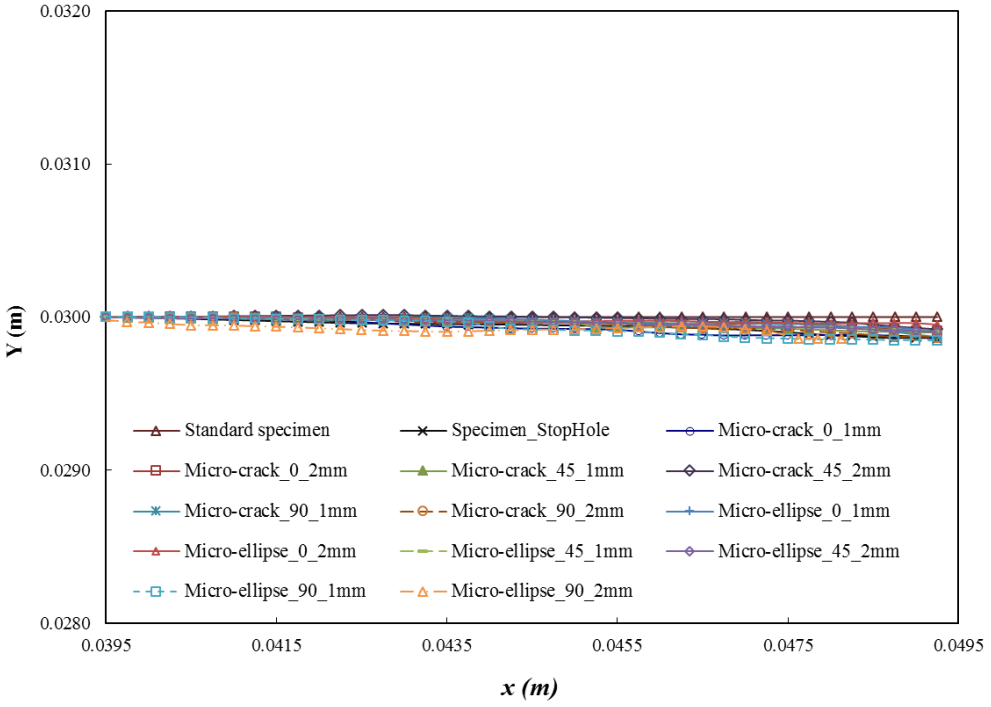

Figure 10: Fatigue crack growth path of main crack interacting with two micro-cracks/ellipses, for different d_y and θ. The specimen is repaired with stop-hole technique.

For the standard specimen, the micro-crack/ellipse with $\theta = 45$ degrees and $d_y = 1$ mm (Micro-crack_45_1mm and Micro-ellipse_45_1mm) show a big impact on the fatigue crack growth path. Also, the micro-ellipse with $\theta = 0$ degree and $d_y = 1$ mm, Micro-ellipse_0_1mm, show almost the same impact on the main crack growth pattern. In addition, micro-crack with $\theta = 0$ degrees and $d_y = 1$ and 2 mm, Micro-crack_0_1mm and Micro-crack_0_2mm, micro-crack with $\theta = 45$ degrees and $d_y = 2$ mm, Micro-crack_45_2mm, show a little miss-consistency with the other crack growth path patterns. In contrast to the results for standard specimen interacting with micro-cracks/ellipses, the repaired specimen with stop-hole specimen presents quite different behavior. In this case, almost all cases show the same pattern for the crack growth path. The difference between these cases is because of existence of the stop-hole. The stop-hole prevents the transferring of the micro-cracks/ellipses effects to the main crack tip, and hence the main crack tip behaves in such a way there is no micro-cracks/ellipses.

If we look at these two previous figures in micro-scale values, some differences can be seen clearly. Figure 11 to Figure 14 presents the results for standard specimen and repaired specimen with stop-hole, both with micro-cracks/ellipses, respectively. As it said before, the micro-cracks/ellipses have more impact on the standard specimen crack growth path than specimen repaired with stop-hole.

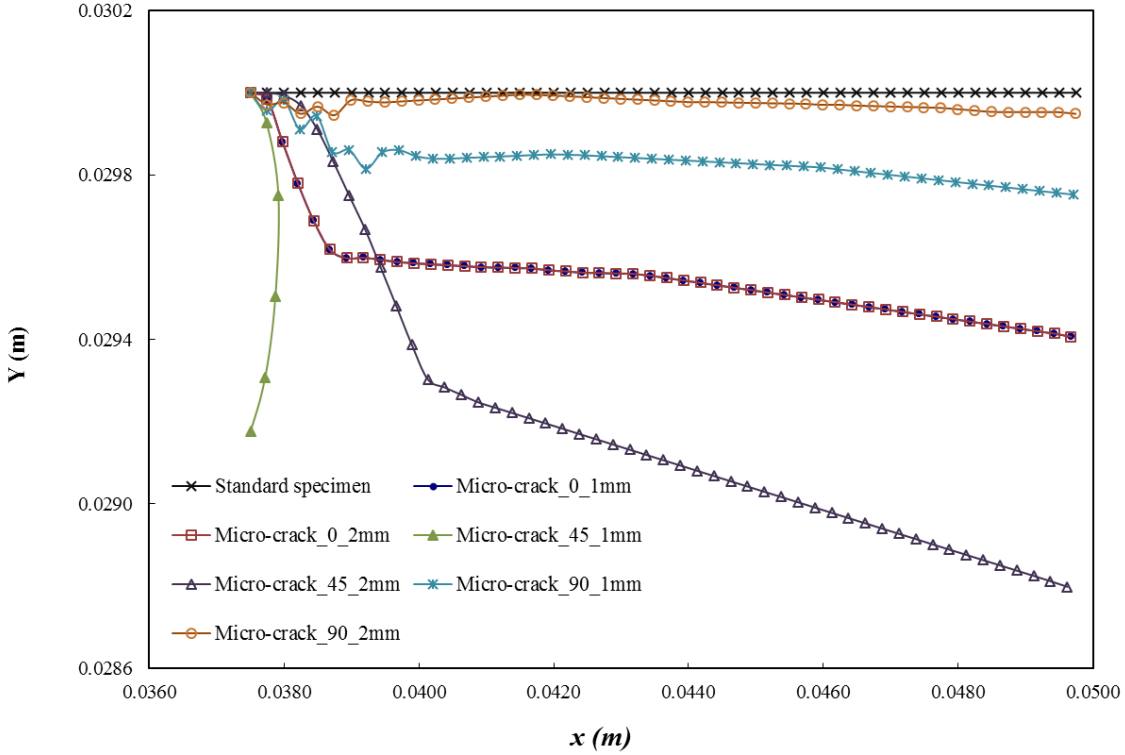

Figure 11: Fatigue crack growth path of main crack interacting with two micro-cracks, for different d_y and θ.

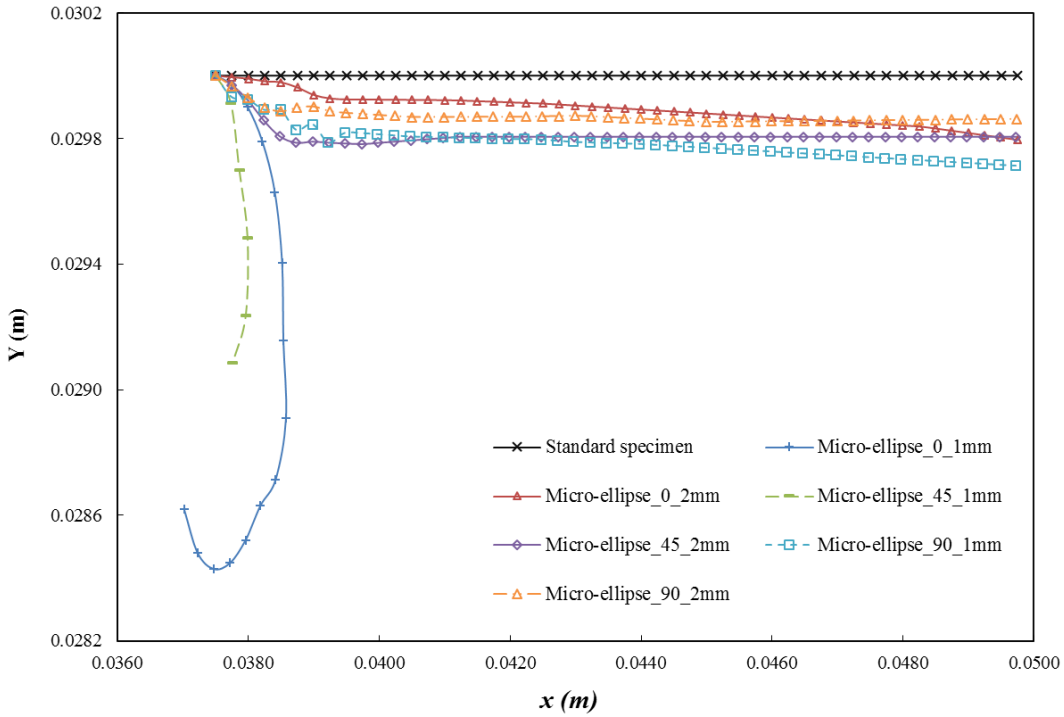

Figure 12: Fatigue crack growth path of main crack interacting with two micro-ellipses, for different d_y and θ.

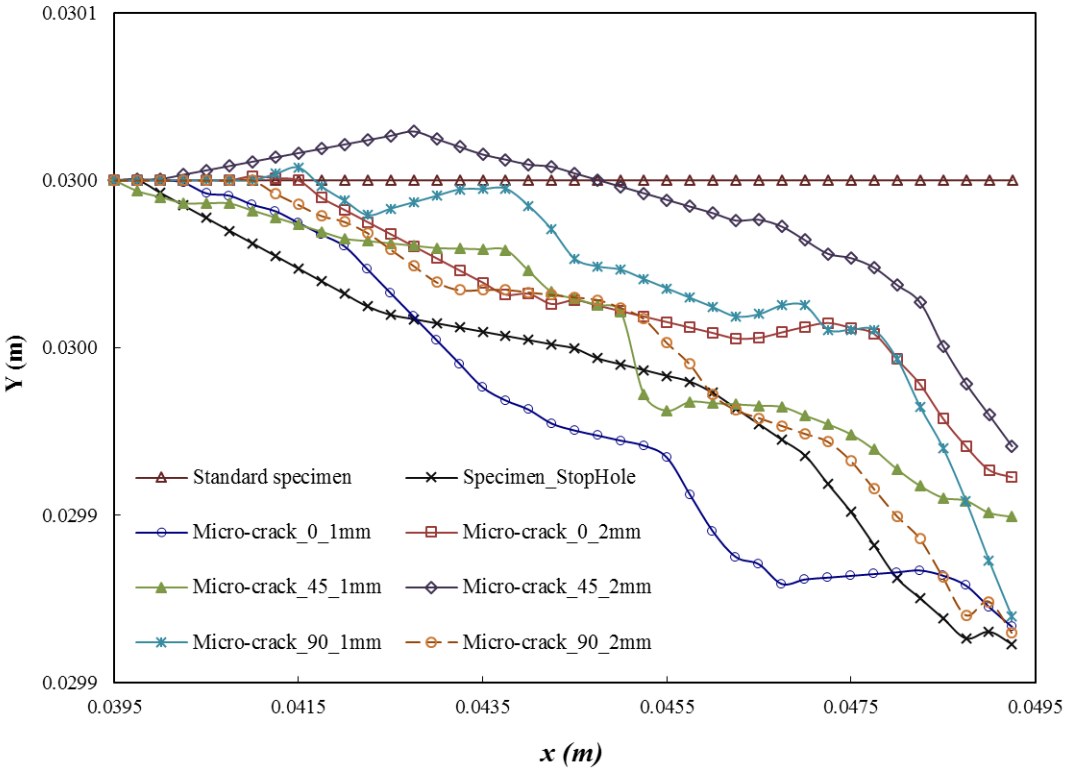

Figure 13: Fatigue crack growth path of main crack interacting with two micro-cracks, for different d_y and θ. The specimen is repaired with stop-hole technique.

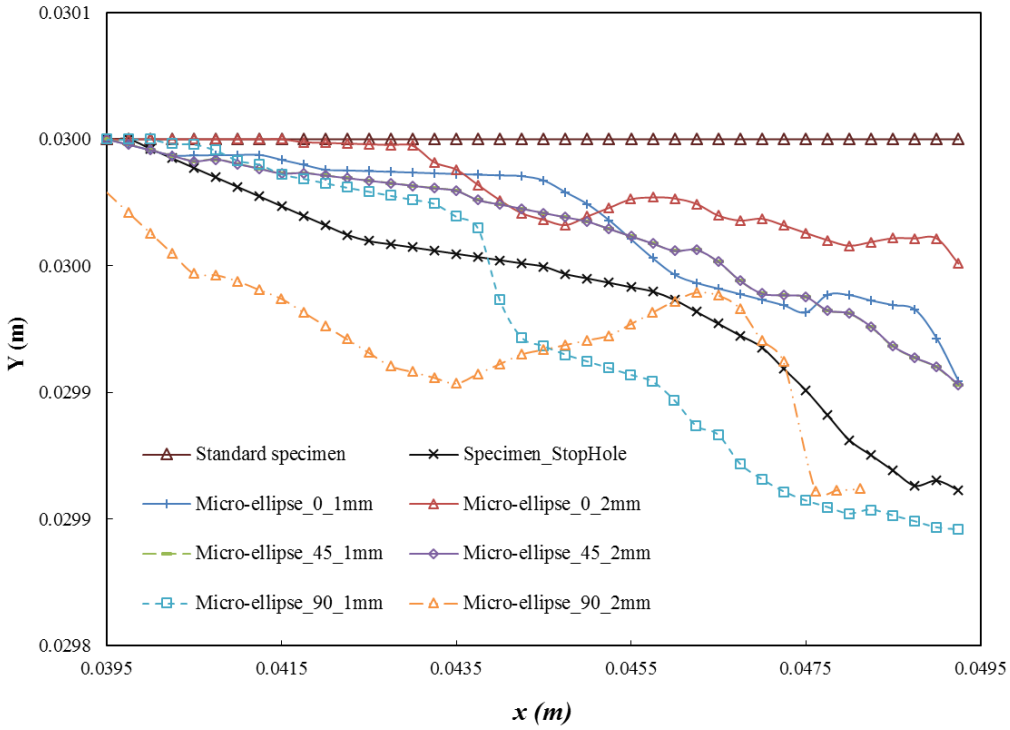

Figure 14: Fatigue crack growth path of main crack interacting with two micro-ellipses, for different d_y and θ. The specimen is repaired with stop-hole technique.

5 CONCLUSION

The main objective of the present study was to observe the effect of stop-hole technique and micro-cracks/voids on fatigue crack propagation behavior of an aluminum compact tension specimen. The numerical results were validated with the analytical and experimental results. On the basis of the present numerical results, the following conclusions are drawn:

- This implementation can accurately capture the fatigue crack growth path using the Paris law equation and available stress intensity factor formulations from the literature.
- Presence of micro-cracks/voids have clear impact on the fatigue crack growth path of the main crack, especially for standard specimen without stop-hole (Figure 9). The micro-cracks have bigger impact than the micro-ellipse. Also, the closer micro-cracks/ellipses to the main crack the more influence on the fatigue crack growth path, for example Micro-crack_45_1mm and Micro-ellipse_45_1mm cases.
- Stop-hole protects the growth path from the influence of the micro-cracks/ellipses. Although, the micro-cracks/ellipses show their effect on the crack growth path for repaired specimen with stop-hole, but the change in the crack growth path is almost negligible, less than 1% deviation from the reference growth path without micro-cracks/ellipses.

This study only considers the effect of two micro cracks/voids on the main crack fatigue crack growth path. Two different positions and three different direction angles were studied here. One of the possible future studies could be modeling more micro-cracks/voids with different distances from the main crack and also different direction angles and analyze their effect on the fatigue crack growth path of the main crack.

ACKNOWLEDGMENTS

The important support of the Brazilian research agencies FAPEMIG (in Portuguese "Fundação de Amparo à Pesquisa do Estado de Minas Gerais"), CNPq and CAPES are gratefully acknowledged.

REFERENCES

[1] Ayatollahi M.R, Razavi S.M.J, Yahya M.Y, (2015) '*Mixed mode fatigue crack initiation and growth in a CT specimen repaired by stop hole technique*', Engineering Fracture Mechanics, 145:115–127.

[2] Song P.S., Shieh Y.L, (2004) '*Stop drilling procedure for fatigue life improvement*', International Journal of Fatigue, 26:1333–1339.

[3] Ghfiri R., Shi H., Guo R., Mesmacque G., (2000) '*Effects of expanded and non-expanded hole on the delay of arresting crack propagation for aluminium alloys*', Materials Science and Engineering, A, 286:244–249.

[4] Shin C.S., Wang C.M., Song P.S., (1996) '*Fatigue damage repair: a comparison of some possible methods*', International Journal of Fatigue, 18(8):535–546.

[5] Ayatollahi M.R, Razavi S.M.J, Chamani H.R, (2014) '*Fatigue life extension by crack repair using stop-hole technique under pure mode-I and pure mode-II loading conditions*', Procedia Engineering, 74:18–21.

[6] Soh A, Yang C, (2004) '*Numerical modeling of interactions between a macro-crack and a cluster of micro-defects*', Engineering Fracture Mechanics, 71:193–217.

[7] Charalambides R, McMeeking P, (1987) '*Finite element method simulation of crack propagation in a brittle microcracking solids*', Mechanics of Materials, 6:71–87.

[8] Chudnovsky A.K.M, Dolgopolsky A, (1987) '*Elastic interaction of a crack with a microcrack array - ii. elastic solution for two crack configurations (piecewise constant and linear approximations)*', International Journal of Solids and Structures, 23(2):11–21.

[9] Hu A.H.Y, Chandra K.X, (1993) '*Multiple void-crack interaction*', International Journal of Solids and Structures, 30(11):1473–1489.

[10] Malekan M, Barros F.B, (2017) '*Numerical analysis of a main crack interactions with micro-defects/inhomogeneities using two-scale generalized/extended finite element method*', Theoretical and Applied Fracture Mechanics (under review).

[11] Bhardwaj G, Singh S, Singh I, Mishra B, Rabczuk T (2016) '*Fatigue crack growth analysis of an interfacial crack in heterogeneous materials using homogenized XIGA*', Theoretical and Applied Fracture Mechanics, 85:294–319.

[12] O'Hara P, Duarte C.A, Eason T (2016) '*A two-scale GFEM for interaction and coalescence of multiple crack surfaces*', Engineering Fracture Mechanics 163:274–302.

[13] Paris P.C, Gomez M, Anderson W, (1961) '*A Rational Analytic Theory of Fatigue*', The Trend in Engineering, 9–14.

[14] Paris P.C, (1963) '*A critical analysis of crack propagation laws*', Journal of Basic Engineering, 85:528–534.

[15] Broek D, (1988) The practical use of fracture mechanics, Kluwer Academic Publishers, Boston, USA.

[16] Hudson C.M, (1969) Effect on in aluminum-alloy of stress ratio fatigue-crack growth 7075-T6 and 2024-T3 specimens, NASA technical note, TN-D-5390, Washington, D.C., USA.

[17] Melson J.H, (2014) Fatigue crack growth analysis with finite element method and a Monte-Carlo simulation, Master of Science dissertation, Virginia Polytechnic Institute and State University, Blacksburg, VA, USA.

[18] Erdogan F, Sih G, (1963) '*On the crack extension in plates under plane loading and transverse shear*', Journal of Basic Engineering, 85:519–527.

[19] Dhondt G, (2014) '*Application of the finite element method to mixed-mode cyclic crack propagation calculations in specimens'*, International Journal of Fatigue, 58:2–11.

[20] Koiter W.T, (1965) '*Rectangular tensile sheet with symmetric edge cracks*', Transactions of ASME, Journal of Applied Mechanics, Series E, 32:237.

[21] Giner E, Sukumar N, Tarancon J.E, Fuenmayor F.J, (2009) '*An Abaqus implementation of the extended finite element method*', Engineering Fracture Mechanics, 76:347–368.